

Baryon Production in the Central Region of Ultrarelativistic Heavy-Ion Collisions

K. Werner

Physics Department, Brookhaven National Laboratory, Upton, New York 11973

(Received 13 February 1989)

We introduce a new string model (VENUS 2) for ultrarelativistic heavy-ion collisions, based on color exchange between quarks and also between antiquarks. These two mechanisms affect the rapidity distribution of baryons differently: Quark color exchange shifts baryons towards central rapidity; antiquark color exchange moves baryons back towards large (c.m.) rapidities. We obtain almost flat baryon rapidity distributions for symmetric $A+A$ collisions. Rapidity distributions for proton-nucleus collisions show a forward plateau rather than a forward peak, in agreement with data.

PACS numbers: 25.70.Np, 12.40.Aa, 25.40.Ve

The amount of stopping of nucleons in an ultrarelativistic heavy-ion collision is of significant importance, since it is directly related to the baryon density at an early time. The baryon number density, on the other hand, determines the nature of a phase transition of hadrons to quark-gluon matter. Unfortunately, there is no direct measurement of proton rapidity distributions from the present CERN heavy-ion experiments (only slow protons can be identified). Although neither proven experimentally nor theoretically, one often assumes a baryon-free central region. This originates partly from predictions of string models.^{1,2} However, one has to keep in mind that there has been no model so far to predict the proton distribution in pA collisions properly, so the question of baryon production in the central region is still open.

In this paper we are going to sketch the new string model VENUS 2, being more general and more consistent than the original VENUS model³ in the sense that not only is color exchange between quarks considered as a basic reaction mechanism, but also color exchange between antiquarks. In particular, we analyze proton and Λ rapidity distributions, since baryon production is more sensitive to details of the model than pion production. It is possible to select a specific set of parameters so that the model matches the conventional dual parton model (DPM), and we are going to compare this DPM option with the default option. We are especially interested in differences concerning central baryon production. We are going to demonstrate that VENUS is not only more consistent than string models so far (we take DPM as a substitute for them), but it is also able to account much better for the forward rapidity plateau in pA collisions. VENUS also predicts more central baryons in AA collisions.

The VENUS model realizes a nuclear collision in three independent steps:

(i) From geometrical considerations, it is determined which nucleons from projectile and target nucleus collide with each other.

(ii) An individual collision leads to color exchange between quarks and also between antiquarks, these color rearrangements being the origin of color string formation.

tion.

(iii) After all strings have been formed due to color exchange, they are fragmented into observable hadrons by using an iterative fragmentation cascade. The fragmentation is assumed to be the same as in lepton scattering.

The complete separation of string formation and string fragmentation is only justified if projectile nucleons are fast enough to be outside the target already before the hadronization (of leading particles) starts. So the hadronization time $\tau_{0\gamma} = \tau_0 \cosh y$ has to be larger than the nuclear dimensions which is easily fulfilled for incident energies of more than 100 GeV per particle. However, even for very high energies there are always slow enough particles produced inside one nucleus.

The nuclear geometry is taken into account by distributing the nucleons inside a nucleus isomorphically according to a Woods-Saxon distribution of the radial coordinate. The nucleons of the two colliding nuclei move on straight lines, making an interaction whenever two nucleons come closer than $(\sigma_{NN}/\pi)^{1/2}$, with σ_{NN} being the inelastic nucleon-nucleon (NN) cross section.

After determining which nucleons collide with each other, we have to specify the nature of the interaction. We assume that an interaction amounts to color exchange either between two quarks or between two antiquarks of the colliding nucleons. The concept of antiquarks participating actively in the interaction is new. So far, we (and other groups) considered only quarks. However, since we were considering not only valence but also sea quarks, it seems to be only consistent to also take into account the antiquarks from the sea.

Let us first repeat the interaction due to quark color exchange.³ Figure 1(a) shows the most important contribution: Color exchange (arrow) between a quark of the projectile and a quark of the target rearranges the singlet structure such that afterwards we find two singlets consisting of a diquark and a quark of the other nucleon. So we have singlets consisting of partons moving (in the NN c.m. system) in opposite directions. Such objects are color strings. Whenever one of the participating quarks is part of a colorless $q\bar{q}$, the situation is some-

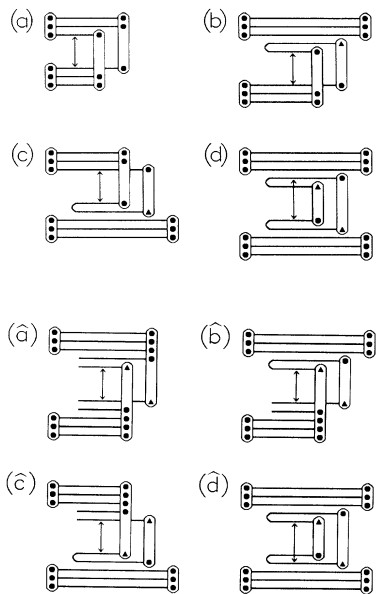


FIG. 1. The basic quark [(a)–(d)] and antiquark [(â)–(dâ)] color-exchange diagrams (see text). Dots are quarks and triangles are antiquarks. Color exchange is indicated by an arrow. Closed q - \bar{q} lines [as in (b)] refer to color-singlet q - \bar{q} pairs, whereas open lines consider a colored q - \bar{q} pair. The closed lines around the quarks and antiquarks indicate this system to be a color singlet. The contributions (â)–(dâ) are just the antiquark analogs of the quark contributions (a)–(d).

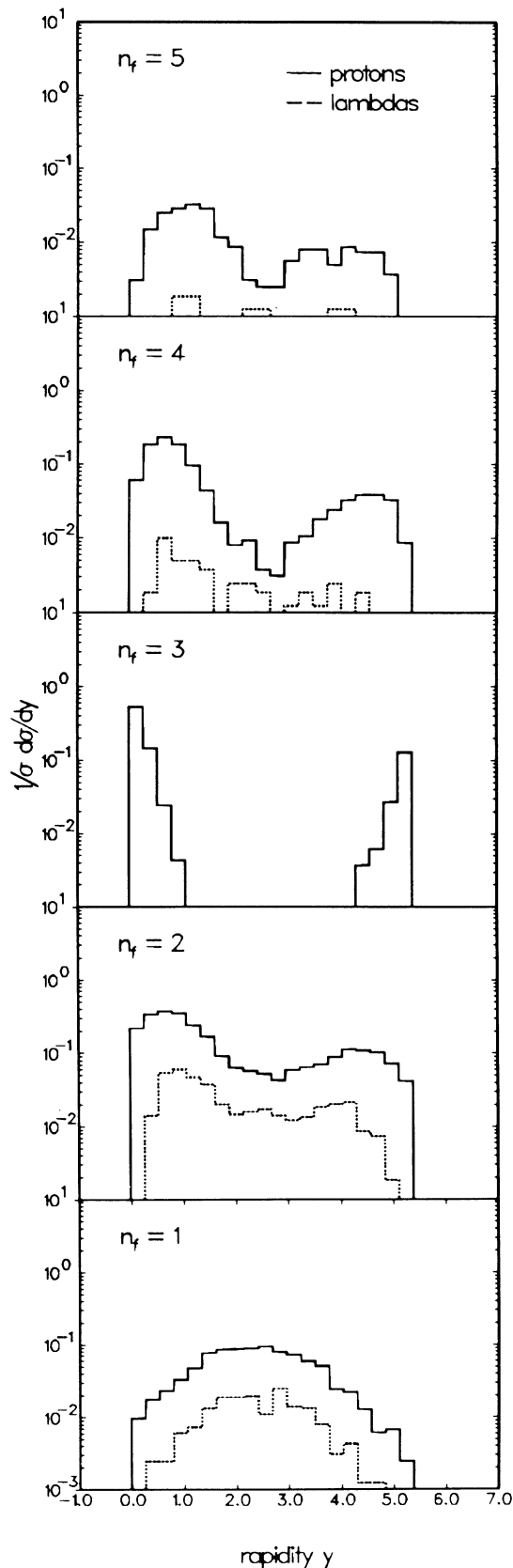
what different, as shown in Figs. 1(b) and 1(c). In this case one q - qq string is replaced by a $q\bar{q}$ string and a baryon (“surviving baryon”). Shown in Fig. 1(d) is the situation where both quarks are part of colorless $q\bar{q}$ pairs, thus leading to two $q\bar{q}$ strings and two surviving baryons. As discussed in Ref. 3, we refer to the contributions of (a)–(d) from Fig. 1 as (a) nondiffractive, (b) and (c) diffractive excitation, and (d) double Pomeron exchange. The probabilities for these contributions are $(1-w)^2$, $w(1-w)$, $(1-w)w$, and w^2 , with w being a parameter which has been fixed to give the correct diffractive cross section.

For simplicity we have plotted in Fig. 1(a), for example, only valence quarks; however, in all calculations we consider sea quarks as well. In this case, the diquark (qq) has to be replaced by a $qq\bar{q}$ system, having, however, the same baryon number as a diquark. Once considering sea quarks, one has, to be consistent, also to consider the antiquarks from the sea. The simplest case of color exchange between antiquarks is shown in Fig. 1(â). This is the antiquark’s counterpart of the nondiffractive quark-exchange contribution (a). The open left ends of the quark (dot) and antiquark (triangle) line in Fig. 1(â) indicate that we are dealing with a q and a \bar{q} that are not a singlet [in the case of a singlet the two lines are closed, see Figs. 1(b)–1(d)]. Color exchange between two antiquarks (triangles) rearranges the singlet structure such

that two strings are formed, each consisting of an antiquark on one end and a quadruquark on the other (\bar{q} - $qqqq$ string). The antiquark contributions corresponding to quark-exchange contributions (b), (c), and (d) are shown in Figs. 1(b̂), 1(ĉ), and 1(d̂).

The relative weights of quark and antiquark color-exchange functions are determined from quark and antiquark structure functions. Also, the string properties like rapidity and mass are calculated from structure functions, as discussed in Ref. 3. The fragmentation of strings into observable hadrons, also described in Ref. 3, has to be generalized, since new types of strings occur, such as \bar{q} - $qqqq$ strings. However, the concept of “spectator-quark counting”³ can be generalized in a quite straightforward manner.⁴

The difference between the quark and antiquark color-exchange diagrams is that quark-diquark (q - qq) strings are replaced by antiquark-quadruquark (\bar{q} - $qqqq$) strings. The number of strings remains the same, and even the baryon-number content of the strings remains the same, but the distribution of baryon number is different. Compared to the baryon number of the baryon before the interaction ($B=1$), the baryon number of the “fast end” of the string has decreased by $\frac{1}{3}$ in the case of quark color exchange and has increased by $\frac{1}{3}$ after antiquark color exchange. Correspondingly, this increase (decrease) of baryon number at the fast end is compensated for by a decrease (increase) of baryon number at the other (slow) end of the string. (With “fast” and “slow” we refer to the pp center of mass, so slow covers the central region and fast the projectile or target fragmentation region.) In addition to the possibility of increasing or decreasing the baryon number of projectile and target, there are still the diffractive contributions (b), (c), (d), (b̂), (ĉ), and (d̂) leaving the baryon number constant. So, by considering one nucleon moving through nuclear matter, we have at each interaction the possibility to change the baryon number of the fast end of the string (projectile remnant) by ΔB_f , with ΔB_f being $-\frac{1}{3}$, 0, or $+\frac{1}{3}$ (we denote the baryon number of the fast and slow ends of a string by B_f and B_s , respectively). We can decompose the whole contribution σ coming from baryonlike ($B_f+B_s=1$) strings as (using $n_f=3B_f$) $\sigma=\sum\sigma_{n_f}$, where n_f denotes the contribution coming from strings with n_f quarks–antiquarks at the fast end of the string. For example, $n_f=2$ corresponds to diquark-quark (qq - q) strings; $n_f=3$ are just baryons (from diffractive scattering); $n_f=4$ are quadruquark-antiquark ($qqqq$ - \bar{q}) strings, etc. In Fig. 2 we demonstrate that the rapidity distributions of baryons (protons and Λ ’s) are very different for those different contributions σ_{n_f} in the case of a proton-nucleus collision. We are considering $p+Ag$ scattering at 100 GeV incident energy. We observe for $n_f=3$ (surviving baryons) two proton peaks around the original projectile and target rapidity. These are the so-called “diffractive” peaks, consisting of protons having suffered only diffractive scatter-



ing, leaving the proton unbroken. The contribution $n_f=2$ includes essentially diquark-quark ($qq-q$) strings, the diquark covering the fragmentation region, the quark covering the central region. Correspondingly, baryon production occurs preferentially in the fragmentation regions ($y \lesssim 1.5$ and $y \gtrsim 4$) showing two peaks in those regions for protons as well as for Λ 's. At least proton production in the central region ($1.5 \lesssim y \lesssim 4$) is unlikely. Contrarily, for $n_f=1$ we have only one quark at the fast end of the string, and the diquark on the slow side. Since quarks are much less likely to produce baryons than diquarks,³ we observe, therefore, for protons as well as Λ 's, peaks in the central region. The distributions for $n_f=4$ ($\bar{q}-qqqq$ strings) are similar to $n_f=2$, producing baryons in the fragmentation regions and not in the central region, since the fragmentation of a quadriquark ($qqqq$) into a baryon is assumed to be equivalent to diquark (qq) fragmentation (the number of spectators is the same, namely, one). The contribution for $n_f=5$ ($\bar{q}\bar{q}-qqqqq$) is again similar to $n_f=4$ and $n_f=2$.

To summarize, the different distributions of baryon number in strings with $n_f=1,2,3,4,5$ lead to different baryon rapidity distributions (shown in Fig. 2): two peaks close to the original nucleon rapidities ($y \approx 0$ and $y \approx 5.4$) for the diffractive contribution $n_f=3$, two peaks in the fragmentation regions ($y \lesssim 1.5$ and $y \gtrsim 4$) for $n_f=2,4,5$, and peaks at the central rapidities ($1.5 \lesssim y \lesssim 4$) for $n_f=1$. Adding up all contributions, we obtain the distribution displayed in Fig. 3(a). So the different peaks shown in Fig. 2 just add up to a rather flat distribution at forward and central rapidities ($y \gtrsim 1.5$), a trend which is also suggested by the data^{5,6} also plotted in Fig. 3(a).

VENUS is a generalization of the DPM of Capella and Tran Thanh Van.⁷ By not allowing antiquark color exchange and by not allowing diquark breakup (setting $n_f^{\min}=2$), VENUS is able to emulate the DPM. In the following we refer to this as the DPM option. In Fig. 3(b), we show proton and Λ rapidity distributions for $p+Ag$ at 100 GeV for the DPM option to compare with the VENUS default option shown in Fig. 3(a). Since in the DPM option we have only the triquark and diquark contributions ($n_f=3, n_f=2$) from Fig. 2, but not the central peak, we also observe for the total distributions [Fig. 3(b)] two peaks in the fragmentation regions and a valley in the central region ($1.5 \lesssim y \lesssim 4$). The data seem to suggest a more flat distribution as predicted by the VENUS default version.

After having demonstrated that the VENUS model provides, in agreement with data, much more stopping than

FIG. 2. Proton and Λ rapidity distributions according to VENUS for a 100-GeV $p+Ag$ collision, split into contributions from strings with different baryon-number characteristics. We are considering strings with different numbers n_f of quarks at the fast end of the string (projectile or target remnant).

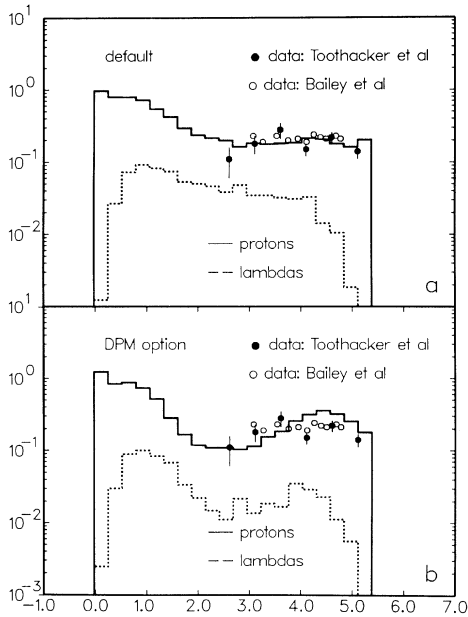


FIG. 3. Proton and Λ rapidity distributions for a 100-GeV p +Ag collision. We plot (a) the VENUS default and (b) the DPM option compared with proton data (Refs. 5 and 6). The DPM option shows much less stopping than the default calculation.

the DPM restriction (see Fig. 3), it is interesting to compare the predictions for nucleus-nucleus collisions. In Fig. 4 we plot baryon rapidity distributions for 200A-GeV S+S collisions, using (a) the VENUS default and (b) the DPM option. It is not very surprising that we observe for the VENUS default option again, as in p +Ag, a plateau for Λ 's and almost a plateau for protons, whereas the DPM option shows two distinct peaks, with quite a deep valley at central rapidity. We observe roughly twice as much proton production in the central region in the VENUS default option compared to DPM, and roughly three times as much Λ production. So the VENUS default results, supported by pA data [Fig. 3(a)], indicate that there is no baryon-free central region in ultrarelativistic heavy-ion collisions.

We have introduced a new string model for ultrarelativistic hadronic collisions, VENUS 2, being more consistent than former versions and other models by also considering color exchange between antiquarks. Quark color exchange amounts to decreasing the baryon number of projectile or target remnant by $\frac{1}{3}$; antiquark color exchange provides an increase by $\frac{1}{3}$. This amounts to shifting the baryon number towards the central region or back towards the fragmentation region. Performing several collisions amounts to a random walk of baryon number in rapidity, adding up to flat baryon rapidity dis-

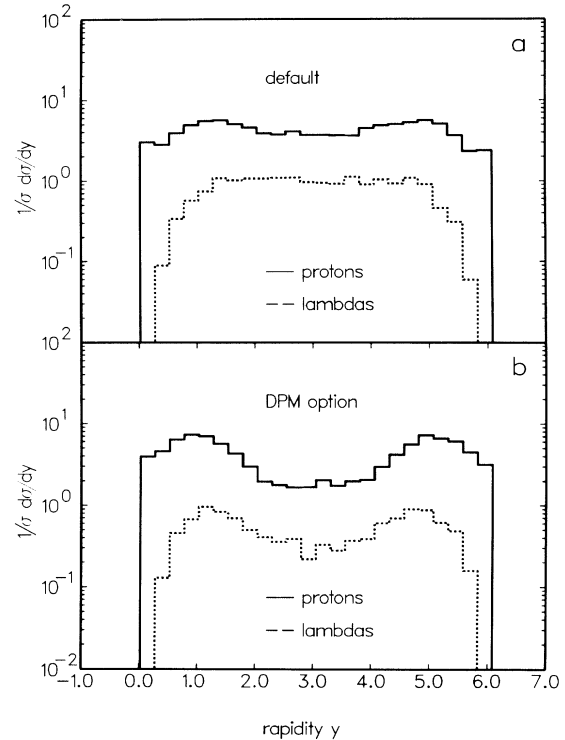


FIG. 4. Proton and Λ rapidity distribution for a central S+S collision at 200A GeV. (a) VENUS default results; (b) DPM option. VENUS default option produces roughly twice as many protons and three times as many Λ 's in the central region, compared to DPM.

tributions for pA as well as AA collisions. At least, pA data also indicate such a plateau. There is no baryon-free central rapidity region.

I acknowledge helpful discussions with P. Koch and S. Kahana. This work has been supported under Contract No. DE-AC02-76CH00016 with the U.S. Department of Energy.

¹B. Anderson, G. Gustafson, and B. Nielsson-Almqvist, Nucl. Phys. **B281**, 289 (1987); M. Gyulassi, CERN Report No. CERN-TH 4794/87 (unpublished).

²J. Ranft and S. Ritter, Z. Phys. C **27**, 413 (1985); J. P. Pansart, Nucl. Phys. **A461**, 521c (1987).

³K. Werner, Phys. Lett. B **208**, 520 (1988); Z. Phys. C **42**, 85 (1989).

⁴K. Werner (to be published).

⁵R. Bailey *et al.*, Z. Phys. C **29**, 1 (1985).

⁶W. S. Toothacker *et al.*, Phys. Lett. B **197**, 295 (1987).

⁷A. Capella, J. A. Casado, C. Pajares, A. V. Ramello, and J. Tran Thanh Van, Z. Phys. C **33**, 541 (1987).